

# VIP-MIXER: A CONVOLUTIONAL MIXER FOR VIDEO PREDICTION

Xin Zheng<sup>1</sup>   Ziang Peng<sup>2</sup>   Yuan Cao<sup>1</sup>   Hongming Shan<sup>3</sup>   Junping Zhang<sup>1,†</sup>

<sup>1</sup> Shanghai Key Lab of Intelligent Information Processing, School of Computer Science

<sup>2</sup> Department of Aeronautics and Astronautics

<sup>3</sup> Institute of Science and Technology for Brain-inspired Intelligence  
Fudan University, Shanghai 200433, China

## ABSTRACT

Video prediction aims to predict future frames from a video’s previous content. Existing methods mainly process video data where the time dimension mingles with the space and channel dimensions from three distinct angles: as a sequence of individual frames, as a 3D volume in spatiotemporal coordinates, or as a stacked image where frames are treated as separate channels. Most of them generally focus on one of these perspectives and may fail to fully exploit the relationships across different dimensions. To address this issue, this paper introduces a convolutional mixer for video prediction, termed ViP-Mixer, to model the spatiotemporal evolution in the latent space of an autoencoder. The ViP-Mixers are stacked sequentially and interleave feature mixing at three levels: frames, channels, and locations. Extensive experiments demonstrate that our proposed method achieves new state-of-the-art prediction performance on three benchmark video datasets covering both synthetic and real-world scenarios.

**Index Terms**— Video prediction, spatiotemporal learning, mixer

## 1. INTRODUCTION

The ability to predict future images by learning from historical contexts provides visual clues for humans and artificial intelligent systems to make judicious decisions in various situations, such as weather forecasting [1], robotic control [2] and autonomous driving [3]. Due to its wide range of applications, video prediction has attracted growing research interests recently [4]. However, it remains challenging to develop video prediction models with the capability to learn complex dynamics, *e.g.*, motions and deformations, while maintaining pixel-level details for high-resolution synthesis [5, 6, 7].

Typically, the appearance of the time dimension is a key difference between video processing approaches and their image counterparts. Therefore, according to how this dimension is treated, we may divide recent works into three categories.

The first category is named as multi-frame modeling, where time is regarded orthogonal to the image-level space

and channel dimensions. Since videos are inherently sequences of frames, it is natural to first extract single-frame features and then mix them across all timesteps using recurrent neural networks (RNNs). PredRNN [8] proposes the ST-LSTM unit and the spatiotemporal memory flow to keep state transitions consistent across time and space at different levels. Following this work, PhyDNet [5] introduces PhyCell to impose physical constraints, while MotionRNN [6] utilizes MotionGRU to learn the transient variations and trending momentum to explicitly represent motions.

In contrast, methods in the second category view videos as tensors. They treat space and time equally via operations such as 3D convolution and patch embedding: FutureGAN [9] builds a 3D convolutional network to perceive spatial and temporal contents at the same time. Inspired by Video Vision Transformer (ViViT) where a clip of video is divided into multiple volumes (patches) [10], EarthFormer [11] proposes a hierarchical Transformer based on Cuboid Attention, where the input tensor is decomposed into cuboids with a certain span in the height, width and time dimensions. We may call this category tensor modeling.

The last category, “image” modeling, seems to be the most straightforward one, which takes time as another form of channel and simply stacks them together so that techniques for images can be applied. For example, SimVP [12] presents a purely 2D convolutional baseline and shows competitive performance as more complex models. It is further improved with the Temporal Attention Unit (TAU) [13] to focus on both intra- and inter-frame correlations, which leads to state-of-the-art results on several benchmarks.

Although we admire the significant advancements made by these pioneering works, we notice that the time dimension merely serves as space, channel or time itself separately in the previous literature, and there are few attempts to integrate these three viewpoints in a unified way. Inspired by feature mixing in MLP-Mixer [14], we propose the **Video Prediction Mixer** (ViP-Mixer), which is composed of Space-Channel (SC) Mixer, Space-Time (ST) Mixer and Time-Channel (TC) Mixer to recognize cues in different combinations of dimensions. We stack ViP-Mixers sequentially to build our model,

†: Corresponding author.

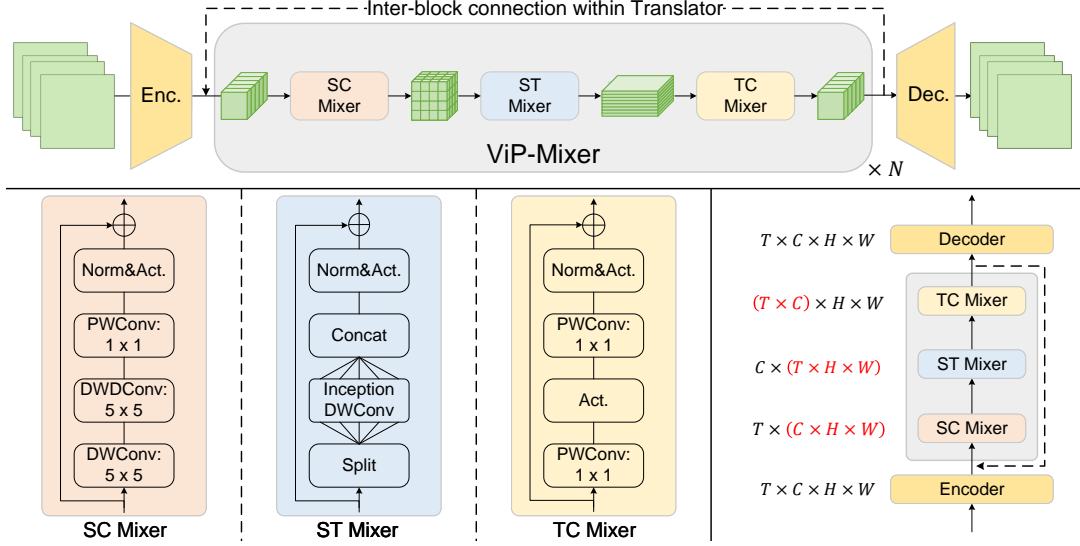


**Fig. 1.** The overall framework of our model and the detailed structures of the proposed ViP-Mixer.

and demonstrate its effectiveness despite its simplicity.

The main contributions of this paper are summarized as follows: 1) we propose ViP-Mixer, a novel module that acquires spatiotemporal relations from three perspectives; 2) we use ViP-Mixers to build a convolutional network for video prediction without any complicated structures or additional tricks; 3) we conduct experiments on synthetic and real-world datasets, and surpass existing works in both qualitative and quantitative evaluations.

## 2. METHODOLOGY

In this section, we introduce ViP-Mixer which models the spatiotemporal evolution in the latent space. The proposed model consists of an encoder, a decoder and multiple ViP-Mixers for information flow across the channel, space and time dimensions.

### 2.1. Network Architecture

The overview of our method is illustrated in Fig. 1. Inspired by SimVP [12] and Latent Diffusion Models (LDMs) [15], we attempt to learn the mapping from past frames to future ones in the latent space, which enables the model to focus on semantic dynamics and also reduces computational demands.

Precisely, given an input sequence of  $T$  images, we denote it as  $\mathcal{X}_{in} = \{x_1, x_2, \dots, x_T\}$ , where  $x_t \in \mathbb{R}^{C \times H \times W}$  is the  $t$ -th frame with channel  $C$ , height  $H$  and width  $W$ . The encoder  $\mathcal{E}$  encodes each frame  $x_t$  into its latent representation  $z_t = \mathcal{E}(x_t) \in \mathbb{R}^{C' \times H' \times W'}$  and thus outputs  $\mathcal{Z}_{in} = \{z_1, z_2, \dots, z_T\}$ . This embedded video tensor  $\mathcal{Z}_{in} \in \mathbb{R}^{T \times C' \times H' \times W'}$  is then fed into the translator  $\mathcal{T}$  and converted into  $\mathcal{Z}_{out} \in \mathbb{R}^{T' \times C' \times H' \times W'}$ , rep-

resenting the embeddings of the  $T'$  subsequent frames. Finally, the decoder  $\mathcal{D}$  reconstructs the predicted pictures  $\mathcal{X}_{out} = \{x_{T+1}, x_{T+2}, \dots, x_{T+T'}\}$  from  $\mathcal{Z}_{out}$  frame by frame. It should be noted that the encoder and the decoder consist of 2D convolutional layers and only take spatial appearances into account, while the translator leverages ViP-Mixers to learn spatiotemporal dynamics underlying the 4D tensor  $\mathcal{Z}_{in}$ .

### 2.2. ViP-Mixer

ViP-Mixer, which originates from MLP-Mixer [14] that contains channel mixing and token mixing operations, is the basic building block of the translator  $\mathcal{T}$ . Similarly, it can be divided into three components: the per-timestep mixer (SC Mixer), the per-channel mixer (ST Mixer) and the per-location mixer (TC Mixer), as shown in Fig. 1.

**Space-Channel Mixer.** The SC Mixer is responsible for learning spatial features within each frame by mixing them up in the space and channel dimensions, so it can be any operators originally dedicated for images. Since depthwise convolutions give promising results in recent works [13, 16], we employ a depthwise convolution ( $\text{Conv}^{\text{DW}}$ ), a depthwise dilated convolution ( $\text{Conv}^{\text{DW-D}}$ ) and a pointwise convolution ( $\text{Conv}^{\text{PW}}$ ) to maintain a large receptive field while reducing computational costs. Specifically, the SC Mixer separates the input tensor  $\mathcal{H} \in \mathbb{R}^{T \times C' \times H' \times W'}$  into  $T$  individual frames and performs frame-wise operations as follows:

$$\begin{aligned} \mathcal{U}'_t &= \text{Conv}_{1 \times 1}^{\text{PW}}(\text{Conv}_{k' \times k'}^{\text{DW-D}}(\text{Conv}_{k \times k}^{\text{DW}}(\mathcal{H}_t))), \\ \mathcal{U}_t &= \sigma(\text{Norm}(\mathcal{U}'_t)) + \mathcal{H}_t, \end{aligned} \quad (1)$$

where  $\mathcal{H}_t \in \mathbb{R}^{C' \times H' \times W'}$  represents the  $t$ -th frame;  $\text{Conv}_{k \times k}$  means a convolution with its kernel size of  $k \times k$ ;  $\sigma(\cdot)$  is a non-linear activation function, which is ReLU in this paper.

After being processed in parallel, all frames are concatenated to form the output tensor  $\mathcal{U} \in \mathbb{R}^{T \times C' \times H' \times W'}$ .

**Space-Time Mixer.** Inspired by InceptionNeXt [17], we use 3D depthwise convolutions with Inception style, denoted as  $\text{IncepConv}^{\text{DW}}$ , to build the ST Mixer which aims to learn spatiotemporal correlations within each channel. The input tensor  $\mathcal{U}$  is first split into five groups along the channel dimension, and then the  $\text{IncepConv}^{\text{DW}}$  layer applies convolutions with different kernels to them except for an identity mapping. Finally, all those groups are concatenated back together. This process can be formulated as follows:

$$\begin{aligned} \mathcal{V}' &= \text{IncepConv}^{\text{DW}}(\text{Split}(\mathcal{U})), \\ \mathcal{V} &= \sigma(\text{Norm}(\mathcal{V}')) + \mathcal{U}. \end{aligned} \quad (2)$$

**Time-Channel Mixer.** The TC Mixer is to mix features across the time and channel dimensions. Following the design of MetaFormer [18], we reshape the input tensor  $\mathcal{V} \in \mathbb{R}^{T \times C' \times H' \times W'}$  into  $\tilde{\mathcal{V}} \in \mathbb{R}^{(TC') \times H' \times W'}$  by stacking all frames along the channel dimension, and pass it through a two layered MLP (equivalent to  $1 \times 1$  convolutions) which maps  $\mathbb{R}^{TC'} \mapsto \mathbb{R}^{TC'}$  and is shared across all locations:

$$\begin{aligned} \tilde{\mathcal{H}}' &= W_2 \sigma(W_1 \tilde{\mathcal{V}}), \\ \tilde{\mathcal{H}} &= \sigma(\text{Norm}(\tilde{\mathcal{H}}')) + \tilde{\mathcal{V}}, \end{aligned} \quad (3)$$

where  $W_1 \in \mathbb{R}^{r(TC') \times (TC')}$  and  $W_2 \in \mathbb{R}^{(TC') \times r(TC')}$  are learnable parameters with  $r$  being the expansion ratio. Note that the operations mentioned here are performed on the whole stacked “image”, which are different from those performed on a single frame in the SC Mixer.

### 3. EXPERIMENTS

We evaluate our method on three datasets for both synthetic and real-world scenarios:

- Moving MNIST (M-MNIST) [19] contains two digits which are initialized at random locations, move with random velocities and bounce off the boundaries at certain angles. All pixel values are normalized to  $[0, 1]$ .
- TaxiBJ [20] records trajectories of traffic flow in Beijing, showing the inflow and outflow of each region at its corresponding pixel with two channels. All pixel values are normalized to  $[0, 1]$ .
- WeatherBench [21] contains physical quantities like temperature, humidity and wind. According to [22], we regrid the raw data with a spatial resolution of  $5.625^\circ$  and choose the temperature field as the predictand.

Since videos of arbitrary length can be predicted in an autoregressive manner [3], we select the same length of input and output as previous works [12, 13] for fair comparison. The statistics of these datasets are summarized in Table 1.

**Table 1.** Statistics of the M-MNIST, TaxiBJ and WeatherBench datasets.

	$N_{train}$	$N_{test}$	$(C, H, W)$	$T_{in}$	$T_{out}$
M-MNIST	10,000	10,000	(1, 64, 64)	10	10
TaxiBJ	19,627	1,334	(2, 32, 32)	4	4
WeatherBench	324,311	17,495	(1, 32, 64)	12	12

#### 3.1. Qualitative Evaluation

We first compare qualitative results of ViP-Mixer with other approaches on M-MNIST. As shown in Fig. 2, the two digits meet each other at  $t = 10$  and are intertwined from  $t = 12$  to  $t = 14$ , which poses a challenge for long-term predictions. Most of the frames produced by the compared models are not very satisfactory: PhyDNet [5] and TAU [13] generate blurry images, failing to reconstruct the digit ‘6’ or ‘7’ which becomes more distorted and illegible as time progresses; PredRNN [8] performs relatively well, but loses details like the horizontal line through the middle of the digit ‘7’ at  $t = 18$  and  $t = 20$ . In contrast, our model produces clearer images, making accurate predictions of the trajectories of the moving digits while maintaining their shapes after occlusions, which means it captures both the temporal dynamics and the static spatial contents.

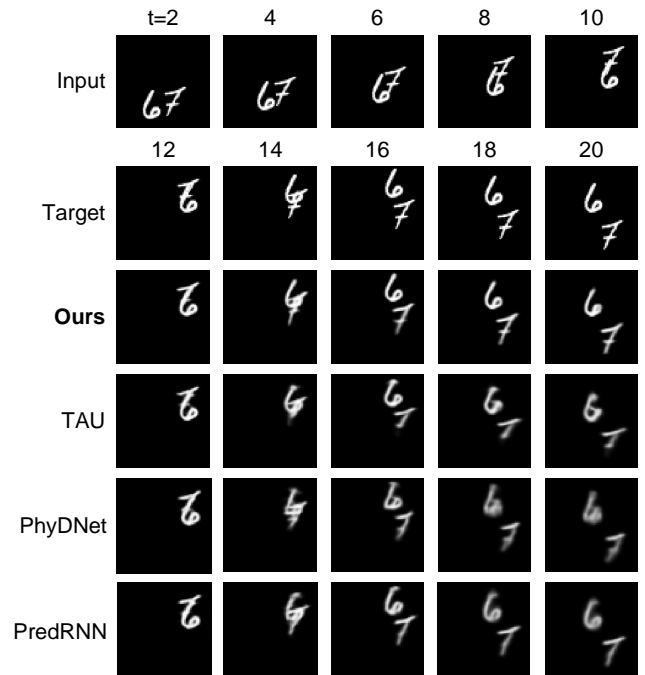


**Fig. 2.** Predicted results on the M-MNIST dataset.

Fig. 3 visualizes an example of our method predicting the traffic flow on TaxiBJ. In this case, the intensity of the traffic flow increases at  $t = 5$ , which may correspond to unexpected congestion during early morning hours. Despite this sudden

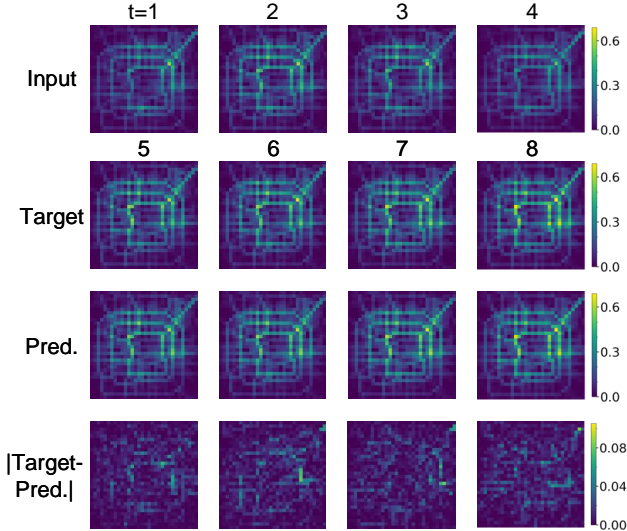


Fig. 3. Predicted results on the TaxiBJ dataset.

change of the traffic flow, ViP-Mixer can still perceive the overall trend and predict the future with high fidelity, demonstrating its practical value in real-world applications.

### 3.2. Quantitative Evaluation

In Table 2, we quantitatively evaluate our proposed method against several strong baselines using the frame-wise Mean Squared Error (MSE), Mean Absolute Error (MAE) and Structural Similarity Index Measure (SSIM). Parameters and FLOPs are also counted as an estimation of model complexity. We see that ViP-Mixer consistently surpasses recent state-of-the-art methods on all benchmark datasets, giving more reliable predictions with less deviation from the ground truth. For example, ViP-Mixer reduces the MSE of currently best TAU [13] on M-MNIST from 20.4 to 17.3, and also brings an improvement of 12.7% for the MAE metric. Meanwhile, it is more parameter-efficient than CNN-based SimVP [12], and consumes less computational resources than RNN-based approaches like PredRNN [8] due to its fully convolutional architecture. These observations further indicate the efficacy of our model.

### 3.3. Ablation Study

We carry out ablation studies on M-MNIST to verify the effectiveness of ViP-Mixer. Comparisons of experimental results in various settings are summarized in Table 3.

Overall, all three kinds of mixers contribute as the absence of any of them degrades the prediction quality. The fusion of the SC Mixer and the ST Mixer (model 1) already provides an efficient baseline exhibiting competitive performance compared with TAU [13]. ViP-Mixer is the product of combining this baseline with the TC Mixer at the cost of more

Table 2. Quantitative results on the three datasets. MSE (MAE) represents the per-frame average MSE (MAE).

Dataset	Method	#Params. (MB)	FLOPs (G)	MSE ( $\downarrow$ )	MAE ( $\downarrow$ )	SSIM ( $\uparrow$ )
M-MNIST	ConvLSTM [1]	15.0	56.8	31.2	92.4	0.927
	PredRNN [8]	23.9	116	24.5	73.8	0.945
	PhyDNet [5]	3.10	15.3	28.7	79.1	0.937
	SimVP [12]	58.0	19.4	25.3	68.9	0.948
	TAU [13]	44.7	15.6	20.4	62.0	0.955
	ViP-Mixer (Ours)	34.6	16.4	<b>17.3</b>	<b>55.4</b>	<b>0.956</b>
TaxiBJ	ConvLSTM [1]	15.0	20.7	0.336	15.3	0.973
	PredRNN [8]	23.7	42.6	0.383	15.6	0.973
	PhyDNet [5]	3.09	5.60	0.362	15.5	0.972
	SimVP [12]	13.8	3.61	0.330	15.1	0.977
	TAU [13]	9.55	2.49	0.333	15.1	0.978
	ViP-Mixer (Ours)	4.04	1.24	<b>0.301</b>	<b>14.7</b>	<b>0.980</b>
Weather Bench	ConvLSTM [1]	14.98	136	1.52	0.794	-
	PredRNN [8]	23.6	279	1.55	0.799	-
	MIM [23]	37.8	109	1.78	0.872	-
	SimVP [12]	14.7	8.03	1.27	0.716	-
	TAU [13]	12.2	6.70	1.23	0.709	-
	ViP-Mixer (Ours)	11.9	7.08	<b>1.18</b>	<b>0.685</b>	-

complexity. On the other hand, only using the TC Mixer to mix per-location features in the time and channel dimensions (model 2) is far from sufficient due to the dearth of spatial contexts. Therefore, either the SC Mixer or the ST Mixer will help it ameliorate the quality of generated frames significantly (model 3 and model 4). The use of all components shows the best result, suggesting that the integration of the three modules, *i.e.*, ViP-Mixer, has the potential to effectively capture the complex dynamics underlying video data.

Table 3. Ablation studies of ViP-Mixer on M-MNIST.

	SC Mixer	ST Mixer	TC Mixer	MSE ( $\downarrow$ )	#Params. (MB)	FLOPs (G)
TAU [13]	-	-	-	20.4	44.7	15.6
model 1	✓	✓	✗	22.5	1.79	8.03
model 2	✗	✗	✓	55.2	33.4	13.3
model 3	✓	✗	✓	18.6	34.3	15.7
model 4	✗	✓	✓	19.3	33.7	14.0
ViP-Mixer	✓	✓	✓	<b>17.3</b>	34.6	16.4

## 4. CONCLUSION

In this paper, we introduce an innovative convolutional network for video prediction. The foundational element of our model is the ViP-Mixer module, which mixes features at the frame-wise, channel-wise and location-wise levels. By stacking these modules as the translator between an encoder and a decoder, the spatiotemporal relationships spanning diverse dimensions are effectively captured. Comprehensive experiments substantiate the superior performance and also the efficiency of ViP-Mixer compared with existing methods.

## 5. REFERENCES

- [1] Xingjian Shi, Zhourong Chen, Hao Wang, Dit-Yan Yeung, Wai-kin Wong, and Wang-chun WOO, “Convolutional LSTM network: A machine learning approach for precipitation nowcasting,” in *NeurIPS*, 2015, vol. 28.
- [2] Chelsea Finn, Ian Goodfellow, and Sergey Levine, “Unsupervised learning for physical interaction through video prediction,” in *NeurIPS*, 2016, vol. 29.
- [3] Vikram Voleti, Alexia Jolicoeur-Martineau, and Chris Pal, “MCVD - masked conditional video diffusion for prediction, generation, and interpolation,” in *NeurIPS*, 2022, vol. 35, pp. 23371–23385.
- [4] Sergiu Oprea, Pablo Martinez-Gonzalez, Alberto Garcia-Garcia, John Alejandro Castro-Vargas, Sergio Orts-Escolano, Jose Garcia-Rodriguez, and Antonis Argyros, “A review on deep learning techniques for video prediction,” *IEEE Trans. PAMI*, vol. 44, no. 6, pp. 2806–2826, 2022.
- [5] Vincent Le Guen and Nicolas Thome, “Disentangling physical dynamics from unknown factors for unsupervised video prediction,” in *CVPR*, 2020, pp. 11474–11484.
- [6] Haixu Wu, Zhiyu Yao, Jianmin Wang, and Mingsheng Long, “MotionRNN: A flexible model for video prediction with spacetime-varying motions,” in *CVPR*, 2021, pp. 15435–15444.
- [7] Zheng Chang, Xinfeng Zhang, Shanshe Wang, Siwei Ma, and Wen Gao, “STRPM: A spatiotemporal residual predictive model for high-resolution video prediction,” in *CVPR*, 2022, pp. 13946–13955.
- [8] Yunbo Wang, Haixu Wu, Jianjin Zhang, Zhifeng Gao, Jianmin Wang, Philip S. Yu, and Mingsheng Long, “PredRNN: A recurrent neural network for spatiotemporal predictive learning,” *IEEE Trans. PAMI*, vol. 45, no. 2, pp. 2208–2225, 2023.
- [9] Sandra Aigner and Marco Körner, “FutureGAN: Anticipating the future frames of video sequences using spatio-temporal 3d convolutions in progressively growing GANs,” *arXiv preprint arXiv:1810.01325*, 2018.
- [10] Christoph Feichtenhofer, haoqi fan, Yanghao Li, and Kaiming He, “Masked autoencoders as spatiotemporal learners,” in *NeurIPS*, 2022, vol. 35, pp. 35946–35958.
- [11] Zhihan Gao, Xingjian Shi, Hao Wang, Yi Zhu, Yuyang (Bernie) Wang, Mu Li, and Dit-Yan Yeung, “Earthformer: Exploring space-time transformers for earth system forecasting,” in *NeurIPS*, 2022, vol. 35, pp. 25390–25403.
- [12] Zhangyang Gao, Cheng Tan, Lirong Wu, and Stan Z. Li, “SimVP: Simpler yet better video prediction,” in *CVPR*, 2022, pp. 3170–3180.
- [13] Cheng Tan, Zhangyang Gao, Lirong Wu, Yongjie Xu, Jun Xia, Siyuan Li, and Stan Z. Li, “Temporal attention unit: Towards efficient spatiotemporal predictive learning,” in *CVPR*, 2023, pp. 18770–18782.
- [14] Ilya O Tolstikhin, Neil Houlsby, Alexander Kolesnikov, Lucas Beyer, Xiaohua Zhai, Thomas Unterthiner, Jessica Yung, Andreas Steiner, Daniel Keysers, Jakob Uszkoreit, Mario Lucic, and Alexey Dosovitskiy, “MLP-Mixer: An all-MLP architecture for vision,” in *NeurIPS*, 2021, vol. 34, pp. 24261–24272.
- [15] Robin Rombach, Andreas Blattmann, Dominik Lorenz, Patrick Esser, and Björn Ommer, “High-resolution image synthesis with latent diffusion models,” in *CVPR*, 2022, pp. 10684–10695.
- [16] Xiaohan Ding, Xiangyu Zhang, Jungong Han, and Guiguang Ding, “Scaling up your kernels to 31x31: Revisiting large kernel design in CNNs,” in *CVPR*, 2022, pp. 11963–11975.
- [17] Weihao Yu, Pan Zhou, Shuicheng Yan, and Xinchao Wang, “InceptionNeXt: when Inception meets ConvNeXt,” *arXiv preprint arXiv:2303.16900*, 2023.
- [18] Weihao Yu, Mi Luo, Pan Zhou, Chenyang Si, Yichen Zhou, Xinchao Wang, Jiashi Feng, and Shuicheng Yan, “Metaformer is actually what you need for vision,” in *CVPR*, 2022, pp. 10819–10829.
- [19] Nitish Srivastava, Elman Mansimov, and Ruslan Salakhudinov, “Unsupervised learning of video representations using LSTMs,” in *ICML*, 2015, pp. 843–852.
- [20] Junbo Zhang, Yu Zheng, and Dekang Qi, “Deep spatiotemporal residual networks for citywide crowd flows prediction,” in *AAAI*, 2017, vol. 31.
- [21] Stephan Rasp, Peter D. Dueben, Sebastian Scher, Jonathan A. Weyn, Soukayna Mouatadid, and Nils Thuerey, “WeatherBench: A benchmark dataset for data-driven weather forecasting,” *J. Adv. Model. Earth Syst.*, vol. 12, no. 11, 2020.
- [22] Cheng Tan, Zhangyang Gao, Siyuan Li, and Stan Z Li, “SimVP: Towards simple yet powerful spatiotemporal predictive learning,” *arXiv preprint arXiv:2211.12509*, 2022.
- [23] Yunbo Wang, Jianjin Zhang, Hongyu Zhu, Mingsheng Long, Jianmin Wang, and Philip S. Yu, “Memory in memory: A predictive neural network for learning higher-order non-stationarity from spatiotemporal dynamics,” in *CVPR*, 2019, pp. 9154–9162.